WILEY

Anti-windup scheme based on 2DOF-PI$^\lambda$D$^\mu$ controller for velocity tracking of linear induction motor

Ameer L. Saleh[1] | Adel A. Obed[2] | Yasir I. A. Al-Yasir[3] ![ORCID] | Issa T. E. Elfergani[4] |
Jonathan Rodriguez[4] | Roger W. Clarke[3] | Raed A. Abd-Alhameed[3]

[1] Department of Electrical Engineering,
College of Engineering, University of
Misan, Misan, Iraq

[2] Electrical Engineering Technical College,
Middle Technical University, Baghdad,
Iraq

[3] School of Electrical Engineering and
Computer Science, University of Bradford,
Bradford, UK

[4] Mobile Systems Group, Instituto de
Telecomunicações, Aveiro, Portugal

Correspondence
Yasir I. A. Al-Yasir, School of Electrical
Engineering and Computer Science,
University of Bradford, Bradford BD7
1DP, UK.
Email: y.i.a.al-yasir@bradford.ac.uk

Summary
Recently, a new scheme of conventional PID (Proportional Integral Derivative)
controller has been utilized in different electrical drives for speed control. This
paper presents an optimal P I$^\lambda$D$^\mu$ controller with 2DOF and anti-windup tech-
niques based on PSO optimization to produce the proposed controller which is
exploited in order to control the velocity control of LIM. A three-phase inverter
with SVPWM technique that is depended on approach of IFOC method is
exploited to obtain the necessary output voltage supplied to the main windings
of the LIM in order to control the velocity with minimum harmonics and good
characteristics. The end effect is taken into account in dq axis equivalent circuit.
Computed investigations show that the proposed controller is efficient in
improving motor performance.

KEYWORDS
2DOF-P I$^\lambda$D$^\mu$ anti-windup, IFOC, linear induction motor, modeling and simulation, PSO algorithm,
SVPWM, velocity control

1 | INTRODUCTION

Recently, LIMs have become very widely utilized in industrial automation like transportation, trains, sliding door
closers, conveyor systems, and elevators, etc. This is because of several outstanding factors, including its operational
high velocity, high starting thrust, simple mechanical structure, mechanical losses reduction and removal of gearing
between the motor and the motion devices, and so on.[1,2] LIM is very beneficial in the applications that required

List of symbols and abbreviations: LIM, linear induction motor; RIM, rotary induction motor; FOC, field-oriented control; IFOC, indirect field
oriented control; VSI, voltage source inverter; PWM, pulse width modulation; SVPWM, space vector pulse width modulation; PI$^\lambda$D$^\mu$, fractional
order PID controller; 2DOF, two degrees of freedom PID controller; PSO, particle swarm optimization; ISE, integral of squared error; M$_p$, overshoot
Nomenclature: V_{ds}, V_{qs}, V_{dr}, and V_{qr}, d-q axes primary and secondary voltages; i_{ds}, i_{qs}, i_{dr}, and i_{qr}, d, q axes primary and secondary currents; λ_{ds},
λ_{qs}, λ_{dr}, and λ_{qr}, d, q axes primary and secondary estimated flux linkage; R_s and R_r, resistance of the primary and secondary windings respectively, per
phase; L_m, L_s, and L_r, mutual, primary, and secondary self-inductances, respectively, per phase; L_{ls} and L_{lr}, primary and secondary leakage
inductances, respectively, per phase; ω_e, ω_r, and ω_{sl}, primary, secondary, and slip electrical frequency, respectively; D, primary length; v, velocity
(m/s); P, number of pole pairs; τ_p, pole pitch; F, electromagnetic thrust force; B, viscous friction; M, total mass of the moving element; K_p,
proportional coefficient; K_i, integral coefficient; K_d, derivative coefficient; λ and μ, integral and derivative order of FOPID; $e(t)$, error of the
output system; $u(t)$, control output; $G(s)$, transfer function; y_{ref} and y, desired and measured values of the output system; w_p, extends from zero
to one; **gbest**, global best position; **lbest**, local best position; **Pbest**, personal best position; x_i^k and v_i^k, instant position and speed of particle i at
iteration k, respectively; w, inertia weight; c_1 and c_2, acceleration constants; R_1, R_2, random variables between 0 and 1; w_{max} and w_{min},
maximum and minimum weights; **iter$_{max}$**, maximum number of iterations; v$_{actual}$, velocity; v$_{ref}$, desired velocity; w, inertia weight factor; c_1 and
c_2, , acceleration constant

linear movement because it produces thrust directly. The LIM is obtained by cutting and opening out rotary IM. The linear motor gives a linear force, which is called thrust rather than producing rotary torque from a RIM. The LIM equivalent circuit is not simply as a RIM owing to the influence of the end effect. The equivalent q-axis electrical circuit for the LIM is as same as the q-axis electrical circuit for a RIM if end effects are not considered. While the end effects are influenced for the period of entrance and exits from the linor, with reference to the primary, the equivalent d-axis electrical circuit in the RIM circuit may not be employed within the investigation of a LIM, while considering the end effects. [2,3]

In most applications of the LIM, a short primary and infinite linor (secondary) are used, where the primary constantly moving in a different secondary area leads to hold an unforeseen increasing of the magnetic flux permeation by authorizing a progressive aggregation of the density of magnetizing field the gap. [2] The main concept of operation of LIM is similar to that of the RIM, but the difference in the internal characteristics is due to the end effect which requires more complicated control and varying of the parameters. [4] In recent years, the developments in the control strategies led to the investigation of several control techniques to control the speed of the motors. One of the control techniques that were used to control the LIM is the FOC technique which is considered as one of the most efficient techniques and provides the similar work as that of separately excited DC machines. [4-7]

A three-phase inverter using SVPWM technique is exploited for controlling the LIM velocity and gets the control signal from the proposed controller based on IFOC method. SVPWM method is widely used to control the motors and inverter applications due to a good performance by minimizing the harmonic contents. [7-9] The IFOC technique is used to separate and control the torque and flux variables using two current controllers and velocity controller depending on the proposed controller.

In this paper, an optimal 2DOF-P $I^\lambda D^\mu$ controller with anti-windup technique is suggested in order to manage the velocity of the LIM using algorithm of PSO by learning the factors of the proposed controller. The function of this controller reduces the output error and gives better response under operating conditions. The Simulink models of linear induction motors are built in Matlab/Simulink. The computed outcomes depict how the proposed controller is effective with various kinds of operation conditions and provide excellent dynamic performance.

2 | MATHEMATICAL MODEL OF LIM DRIVE SYSTEM

2.1 | Mathematical model of LIM

The three-phase LIM dynamic model is comparable to the dynamic model of the rotary three phase IM but is different in respect of the influence of the end effect, where the end effect of LIM increases with increasing the velocity of the motor and thus has an influence on the direct axis equivalent circuit, but the quadrature axis equivalent part is not influenced by end effect and similar to the quadrature axis equivalent rotary IM. [4,6] Figure 1 shows the dq-axis circuit; the end effect is being taken into account.

From the d-q equivalent circuit, the voltage equations can be described in a synchronous reference system as [3-8]

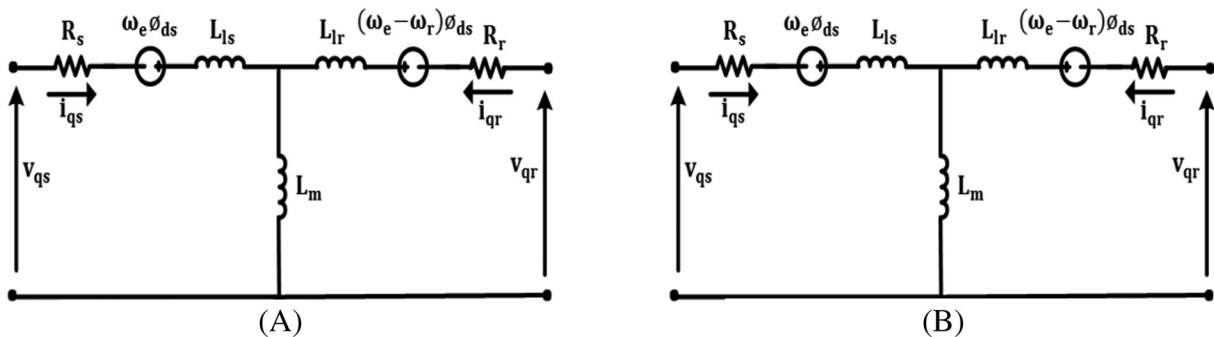$$V_{ds} = R_s i_{ds} + R_r f(Q) (i_{ds} + i_{dr}) + p\lambda_{ds} - \omega_e \lambda_{qs} \tag{1}$$

FIGURE 1 The equivalent circuits of LIM. A, d-axis; B, q-axis

$$V_{qs} = R_s\, i_{qs} + p\lambda_{qs} + \omega_e\lambda_{ds} \tag{2}$$

$$V_{dr} = R_r i_{dr} + R_r f(Q)\, (i_{ds} + i_{dr}) + p\lambda_{dr} - \omega_{sl}\lambda_{qr} \tag{3}$$

$$V_{qr} = R_r\, i_{qr} + p\lambda_{qr} + \omega_{sl}\lambda_{dr} \tag{4}$$

where the flux linkages of the primary and secondary are expressed as

$$\lambda_{ds} = L_{ls}\, i_{ds} + L_m(1 - f(Q))\, (i_{ds} + i_{dr}) \tag{5}$$

$$\lambda_{qs} = L_{ls}\, i_{qs} + L_m\, (i_{qs} + i_{qr}) \tag{6}$$

$$\lambda_{dr} = L_{lr}i_{dr} + L_m(1 - f(Q))\, (i_{ds} + i_{dr}) \tag{7}$$

$$\lambda_{qr} = L_{lr}i_{qr} + L_m\, (i_{qs} + i_{qr}). \tag{8}$$

From the abovementioned formulas, the influence of the end effect can be described as

$$f(Q) = \frac{1 - e^{-Q}}{Q} \tag{9}$$

where,

$$Q = \frac{D\, R_r}{(\, L_m + L_{lr})\, v}. \tag{10}$$

While the end effect is a function of the primary length and velocity of the motor. Therefore, the magnetization inductance is changed with changing the end effect as

$$L_m' = L_m\, (1 - f(Q)). \tag{11}$$

The thrust force is given by

$$F_e = \frac{3\pi P}{2\tau_p 2}(\lambda_{ds}i_{qs} - \lambda_{qs}i_{ds}) = M.v' + B.v + F_L. \tag{12}$$

2.2 | Indirect field oriented control (IFOC)

The IFOC approach depends on separating the control of torque and variables of flux in the machine, which could obtain a similar act to that of an independently excited DC machine. The concept of IFOC technique aims at controlling the stator currents by conveying the currents of three phase using the electrical positioning of LIM to get the current of two phase in the d-q reference structure scheme. This results in separating the flux and the torque variables and then controls the stator direct-axis current i_{ds} and quadrature-axis current i_{qs} independently.[4,6,7]

The IFOC scheme utilizes the measured velocity of LIM to control the velocity using the controller of velocity, which provides the reference quadrature-axis current i_{qs} for controller of current that is then compared with the feedback quadrature-axis current i_{qs} to get the necessary voltage v_q for the SVPWM inverter for controlling the torque. While the flux can be controlled using the current controller to control direct-axis current i_{ds}, by comparing the reference direct-axis current i_{ds} to the direct-axis current feedback i_{ds} to obtain the required voltage v_d.[6,7] Within the IFOC, LIM secondary flux linkage axis should be in line together with the d-axis, and the field orientation conditions can be described as

$$\lambda_{qr} = p\lambda_{qr} = 0 \tag{13}$$

$$\lambda_{dr} = \lambda_r = L_m\, i_{ds}. \tag{14}$$

Moreover, Equations (13) and (14) can be combined with Equation (12) to obtain the thrust force equations as

$$F_e = k_f\, . i_{qs} \tag{15}$$

$$F_e = \frac{3\pi}{2\tau_p} P \frac{L_m(1 - f(Q))}{(L_r - L_m f(Q))}\lambda_{dr}. \tag{16}$$

Equations (13) and (14) can be combined with Equation (3) to obtain the feed-forward slip velocity signal as

$$v_{sl} = \frac{\tau_p . L_m(1 - f(Q)).i_{qs}{}^*}{\pi.\left(\dfrac{L_r}{R_r} - \dfrac{L_m f(Q)}{R_r}\right).\lambda_{dr}}. \tag{17}$$

Whereas, the electrical velocity is defined by the equation

$$v_e = v_{sl} + v_r. \tag{18}$$

The technique of decoupling control utilizing dual current controllers, which have been employed to supply the necessary controlling voltages to the inverter, may be stated as

$$V_{ds}{}^* = (\text{current controller})\left(i_{ds}{}^* - i_{ds}\right) - \frac{\pi}{\tau_p}v_e L_\sigma(Q)\, i_{qs}{}^* \tag{19}$$

$$V_{qs}{}^* = (\text{current controller})\left(i_{qs}{}^* - i_{qs}\right) + \frac{\pi}{\tau_p}v_e L_\sigma(Q)\, i_{ds}{}^* + \frac{P.L_m}{L_r}\frac{\pi}{\tau_p}v_r\, \lambda_{dr}. \tag{20}$$

Whereas, the controller velocity could be stated represented as follows:

$$i_{qs}{}^* = (\text{Speed Controller})\left(v_r{}^* - v_r\right) \tag{21}$$

where $i_{qs}{}^*, i_{ds}{}^*$ are the reference d-q axis of the secondary currents, and $v_r{}^*$ is the reference velocity; $L_\sigma(Q)$ is the leakage inductance with influence on the end effect, which can be expressed as

$$L_\sigma(Q) = L_s - L_m\, f(Q) - \frac{(L_m(1 - f(Q)))^2}{L_r - L_m f(Q)}. \tag{22}$$

2.3 | VSI-based SVPWM technique

The voltage of three-phase VSI is utilized to deliver the essential voltage and frequency to the three-phase LIM according to the control method. A SVPWM method is employed for the inverter controlling by providing the required switching signals to it. The SVPWM technique was modified from the PWM technique for the three-phase inverter using representation of space vector for in the α-β plane.[9,10] The stationary α-β reference frame is accomplished when the transformation of three-phase voltages takes place by Clarke's transformation. The main concept of SVPWM depends on the special switching sequence of the three-phase inverter. The combination of switches may be characterized as binary codes that coincide with the three-phase inverter power transistors. Table 1[11] states the potential switch with eight states of the inverter. The switching states result in six nonzero vectors (V_1 toV_6) which compose a regular hexagon with six equal sectors phase angle is 60° and two zero vectors (V_0 and V_7) which lies on the origin of the hexagon with zero amplitude as shown in Figure 2.

TABLE 1 The switching and the output voltage of the VSI

Voltage Vectors	Switching Vectors			Phase Voltages			Line Voltages		
	A	B	C	V_{an}	V_{bn}	V_{cn}	V_{ab}	V_{bc}	V_{ca}
V_0	0	0	0	0	0	0	0	0	0
V_1	1	0	0	2/3	−1/3	−1/3	1	0	−1
V_2	1	1	0	1/3	1/3	−2/3	0	1	−1
V_3	0	1	0	−1/3	2/3	−1/3	−1	1	0
V_4	0	1	1	−2/3	1/3	1/3	−1	0	1
V_5	0	0	1	−1/3	1/3	2/3	0	−1	1
V_6	1	0	1	1/3	−2/3	1/3	1	−1	0
V_7	1	1	1	0	0	0	0	0	0
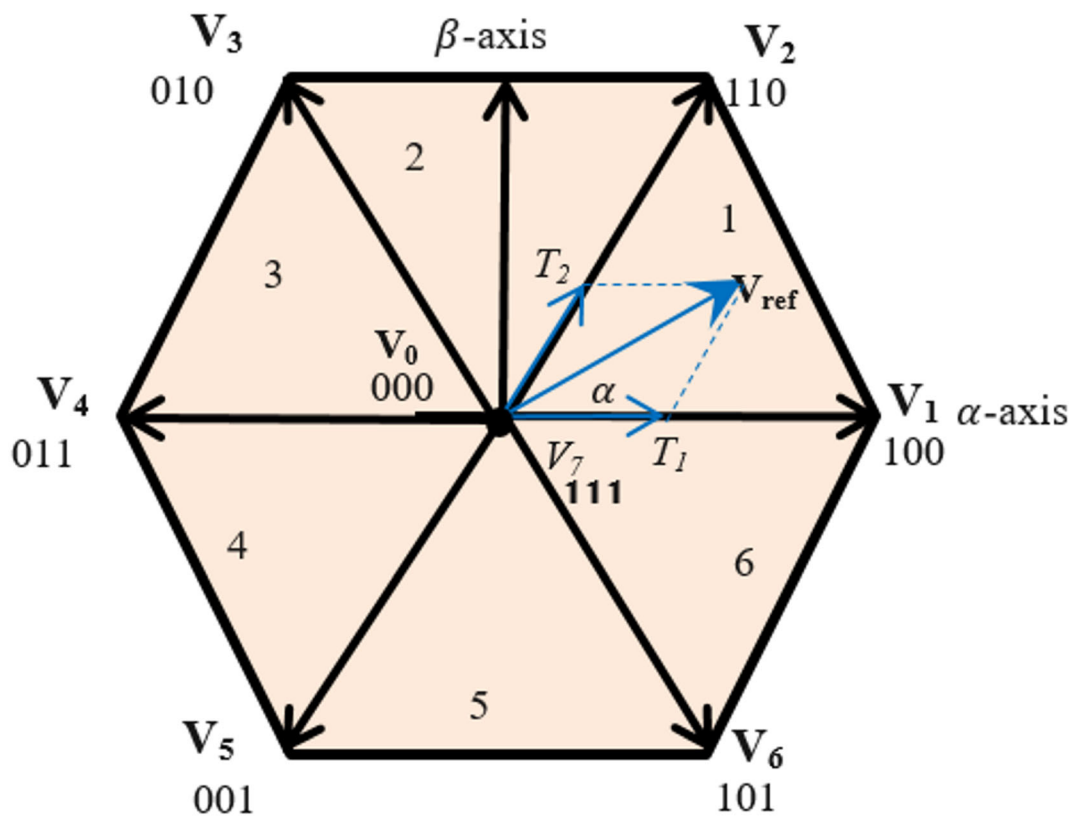
FIGURE 2 Switching vectors and voltage

3 | CONTROL DESIGN

3.1 | Fractional order PID (Proportional Integral Derivative) (PI$^\lambda$D$^\mu$) controller

FOPID controller (P I$^\lambda$D$^\mu$) is an expansion of a conventional PID controller, where derivation and integration order has fractional values. The modified PID (P I$^\lambda$D$^\mu$) controller with a new integral λ and derivative μ orders makes the system less sensitive and more flexible.[12,13] The fractional order of the PI$^\lambda$D$^\mu$ controller is described by the differential equation as

$$u(t) = K_p \ e(t) + K_i \ D^{-\lambda}e(t) + K_d D^\mu \ e(t). \tag{23}$$

While the controller transfer function can be represented by Laplace transform as follow:

$$G(s) = K_p + K_i S^{-\lambda} + K_d S^{\mu}. \tag{24}$$

The generalized block diagram of $PI^{\lambda}D^{\mu}$ controller is indicated in Figure 3. The traditional PID may be obtained by taking $\lambda = 1$, $\mu = 1$. Furthermore classical PD & PI controllers can be produced by taking $\lambda = 0$, $\mu = 1$ and $\lambda = 1$, $\mu = 0$ correspondingly.

3.2 | 2DOF-PID controllers based on anti-windup technique

Two degrees of freedom (2DOF) PID controller is a modified form of the PID controller proposed to overcome the limitations of the classical PID controllers and improving the closed loop system functionality. In addition, it can control both the rejection of disturbance and set point tracking. The modified equation of the 2DOF-PID controller is described as follows. [14-16] The 2DOF PID controller uses the following modified equation[16]:

$$u(t) = k_p \left(w_p y_{ref}(t) - y(t) \right) + k_i \int e(t) dt + k_d \frac{d}{dt} \left(w_d y_{sp} - y(t) \right) \tag{25}$$

where the overshoot of the reference point can be reduced by decreasing w_p without changing the parameters of PID controller and the bounce of the derivative during the reference point change can be removed by making w_d equal to zero. [14,16] The windup phenomenon is occurred due to the saturation in the output of PID controller, which causes the integrator windup, and thus the controller's performance will be decreased. In fact, when the control output signal reaches to the saturation, the closed loop is broken and makes the system operate as an open loop. There are many techniques offered to deal with the effects of a windup occurrence, called anti-windup methods.

In this work, a tracking back-calculation scheme is utilized to overcome the windup phenomenon. This method is exploited for generating a feedback signal to act the integral term during the saturation of the control signal output. In particular, the integral term can be restarted by adding feedback that is produced from the alteration of the saturated and unsaturated control signal with tracking time constant T_t. The input signal to integral term is

$$e_i = k_i e + \frac{1}{T_t}(u - u') \tag{26}$$

where e is the system error; u and u' are the saturated and unsaturated control output signal; and T_t is the tracking time constant which can determine the speed resetting of the integral.

3.3 | 2DOF-P $I^{\lambda}D^{\mu}$ controllers based on anti-windup technique

The 2DOF-$PI^{\lambda}D^{\mu}$ controllers based on anti-windup technique is proposed to control the LIM velocity. In this paper, the new scheme includes three stages: Firstly, 2DOF is used to give greater tolerance in the control system. Secondly, $PI^{\lambda}D^{\mu}$ controller is used to increase the accuracy of the system with better performance and more flexibility. Thirdly, the back
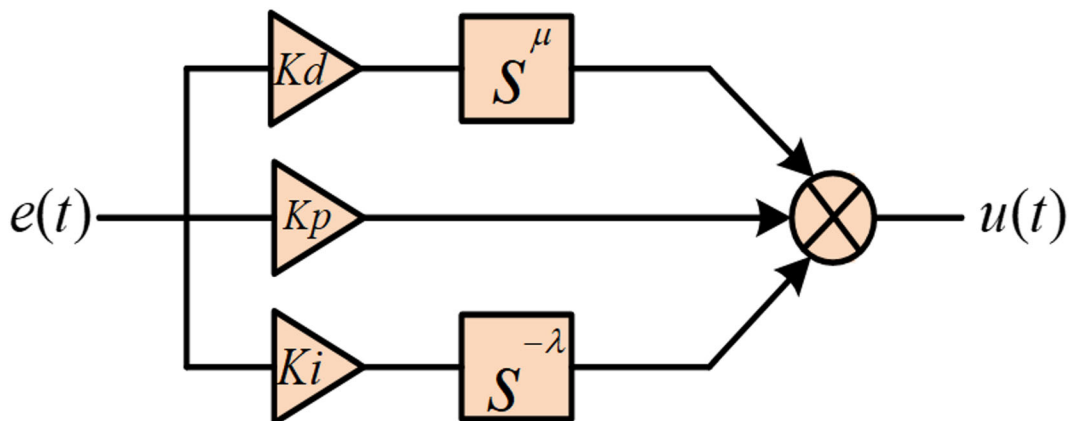

FIGURE 3 Block diagram of FOPID controller

calculation anti-windup method is used to overcome the saturation in the controller output signal. Tracking back calculation is based on recalculating the fractional integral term during linear and saturation range by using limiter such as[15,16]

$$
e_i = \begin{cases} e\,k_i & \text{if } u = u' \\ e\,k_i + \dfrac{1}{T_t}(u - u') & \text{if } u \neq u'. \end{cases} \tag{27}
$$

The differential equation of the $PI^\lambda D^\mu$ is modified according to the 2DOF-PID controller with anti-windup technique to produce the equation of the proposed 2DOF-$PI^\lambda D^\mu$ based on the anti-windup controller as follows:

$$
u(t) = K_p \left(w_p\, y_{ref}(t) - y(t) \right) + K_i\, D^{-\lambda}\, e_i(t) + K_d D^\mu \left(-y(t) \right). \tag{28}
$$

The parameters of the present controller are tuning by utilizing PSO algorithm to give better response for the velocity control. The block diagram of the 2DOF-$PI^\lambda D^\mu$ controller with anti-windup techniques is shown in Figure 4.

3.4 | Algorithm for PSO technique

PSO is an inhabitance based on computational technique motivated by the emulation of gregarious performance of bird flocking, fish schooling, and swarm theory. PSO is a method utilized to explore the search space of a given problem to obtain the best solution according to the particular objective. The technique has been shown to be powerful in solving problems with complex and nonlinear systems, multidimensional and nondifferentiable systems through learning. [6,13]

The algorithm of PSO is one of the evolutionary computation procedures for solving optimization issues. Such technique can be employed for controlling the LIM velocity that includes a particular objective function to give optimal results. In this paradigm, any separate answer is called a particle. Each particle comes up with its own primary velocity that flows in the search space with the issue dimensions. The initial velocity of each particle is constantly updated by both its own prior practice and know-how of adjacent particles in its swarm in order to choose its finest and optimum position that is which entitled the personal best location (called the Pbest). In the case of the particle in the swarm having its ideal position in the swarm, this is named the global best position (gbest). The best prior position for any particle is named the local best position (lbest). The swarm direction of a particle is determined by the set of particles neighboring the particle, and its previous experience to come up with a decision of such ideal solution is achieved in relation to the objective function whereby the best prior location providing the lowest fitness value.

Each particle performance is determined by employing a cost function, which differs relying on the optimization issue.[14,17,18] For a multidimensional issue, the position and velocity of such a single particle in the swarm are obtained by exploiting the following equations:
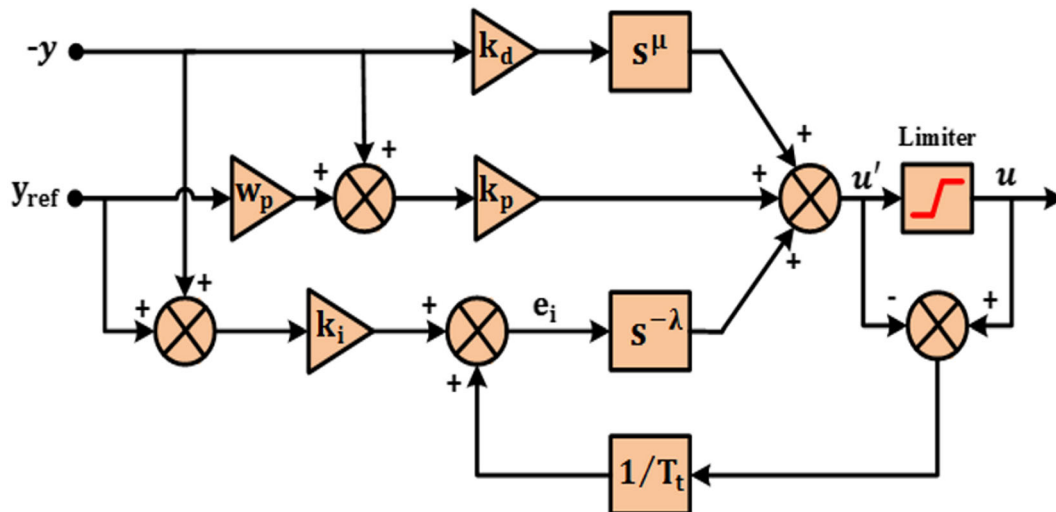

FIGURE 4　Block diagram of the 2DOF-$PI^\lambda\, D^\mu$ with anti-windup

$$v_i^{k+1} = w \, v_i^k + c_1 \, R_1 \, \left(lbest_i - x_i^k\right) + c_2 \, R_1 \left(gbest_i - x_i^k\right) \tag{29}$$

$$x_i^{k+1} = x_i^k + v_i^{k+1} \tag{30}$$

where the weight of each particle can be expressed as

$$w = w_{max} - \frac{\left(w_{max} - w_{min}\right).}{iter_{max}}. \tag{31}$$

Within this work, the advantage of a multicost function is exploited to discover the best results along with less level of velocity error depending on the smallest ISE criterion and minimum M_p criterion as stated[13,15,17]:

$$\text{Fitness function} = \min \, (ISE) + \min\left(M_p\right) \tag{32}$$
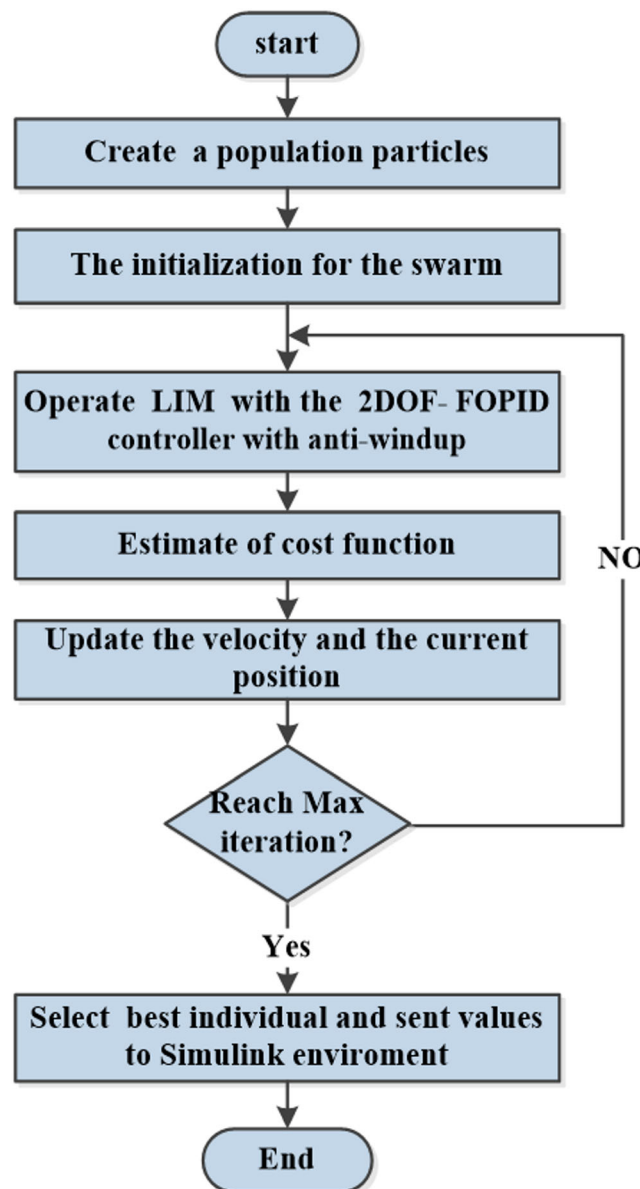
FIGURE 5 Flow chart of the PSO algorithm

where

$$ISE = \int e(t)^2 dt \tag{33}$$

$$M_p = v_{max} - v_{ref} \tag{34}$$

$$e(i) = v(i) - v_{ref}(i). \tag{35}$$

By using transient response and steady state method (relative stability), the proposed controller verifies the stability of the LIM system according to the velocity response.[19-22]

The flow chart of the PSO algorithm can be indicated in Figure 5.

4 | VELOCITY CONTROL OF LIM BASED ON 2DOF-PI$^\lambda$D$^\mu$ CONTROLLER WITH ANTI-WINDUP TECHNIQUE

The main goal of the proposed controller is to control the velocity of the LIM to achieve the set desired velocity. The LIM drive system is controlled via a three-phase inverter based on IFOC method in order to offer the necessary voltages to track the velocity desired. The SVPWM inverter collects the switching signals of the present controller. It is recommended to decrease the switching frequency of the inverter switches.

The control system based on IFOC method comprises the velocity and current of the controller, to achieve a speed and flux tracking. The velocity controller is applied for controlling the velocity of LIM depending on the proposed controller to get the reference velocity with good response. While the current controller contains two loops in order to control the flux of the LIM with the aid of the proposed controller to provide the essential voltage for three-phase inverter.

Within this work, the parameters of the 2DOF- PI$^\lambda$D$^\mu$ controller with anti-windup technique are tuning using PSO algorithm to get better performance than the conventional PID controller. Figure 6 indicated the block diagram of the LIM with online tuning 2DOF-PI$^\lambda$D$^\mu$ controller with anti-windup technique based on PSO algorithm. The PSO parameters which are utilized for learning the mentioned controller to get good performance are as follows:

- Dimension of problem = 7
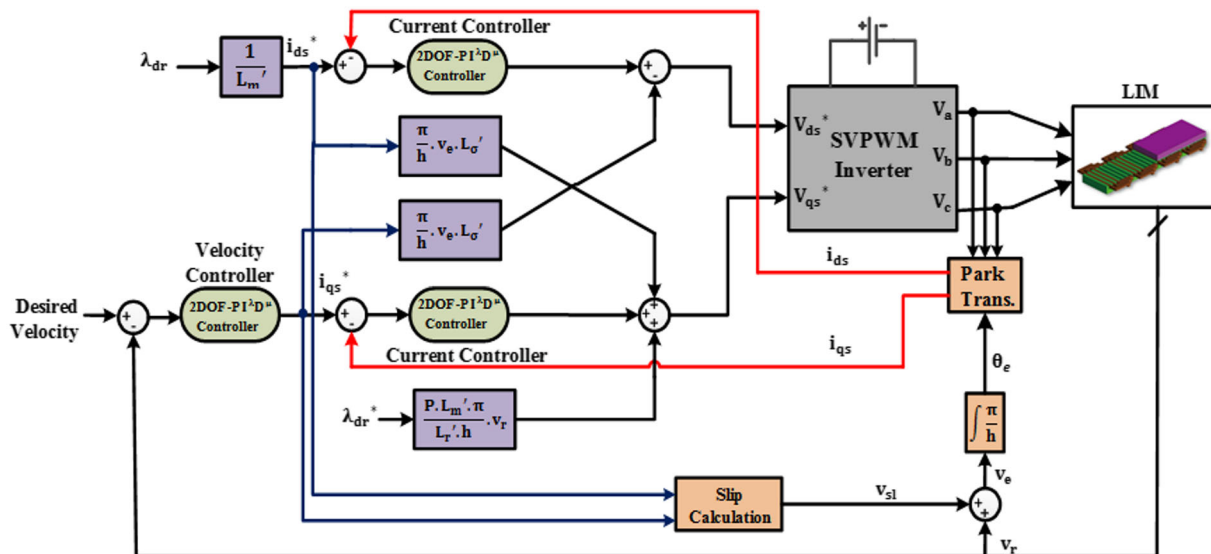- No. of birds =60.
- Maximum iteration number = 40.

**FIGURE 6** Block diagram of LIM with the suggested controller

FIGURE 7 The drive system model of LIM

- $w_{max} = 0.7$ and $w_{min} = 0.3$
- $c_1 = 1.8$ and $c_2 = 2$.

5 | SIMULINK IMPLEMENTATION AND RESULTS

The overall model of LIM drive system with optimal 2DOF- $PI^\lambda D^\mu$ controller with an anti-windup technique based on IFOC method is executed in Simulink/Matlab program indicated in Figure 7. The model of the LIM is implemented according to the given mathematical equations (1-12) as shown in Figure 8. Table 2 shows the parameter values of LIM.[6] After tuning (using PSO algorithm), the optimal coefficient values of the proposed controller are obtained as shown in Table 3.

FIGURE 8 The Simulink model of the LIM

TABLE 2 Parameters of LIM

Parameters	Value	Parameters	Value
R_S (Ω)	13.2	τ_p (m)	0.0465
R_r (Ω)	11.78	M (kg)	4.775
L_S (H)	0.42	P	4
L_r (H)	0.42	B (kg/s)	53
L_M (H)	0.4	λ_r(Wb)	0.056

TABLE 3 Optimal parameters of 2DOF-PI$^\lambda$D$^\mu$ controller

Parameters	Value	Parameters	Value	Parameters	Value
k_{p1}	5.99	k_{p2}	69.89	k_{p3}	2.782
k_{i1}	9.4	k_{i2}	59.94	k_{i3}	0.992
k_{d1}	0.025	k_{d2}	0.0264	k_{d3}	0.00056
λ_1	0.97	λ_2	0.67	λ_3	1.213
μ_1	0.825	μ_2	1.348	μ_3	0.965
w_{p1}	0.936	w_{p2}	0.703	w_{p3}	9.422
T_{t1}	9.31	T_{t2}	8.6	T_{t3}	8.271

The validity of the present controller for controlling the velocity of LIM has been achieved by implementing several tests along with several diverse operating cases; this includes the response of velocity in the no load case and in the scenarios of load (thrust) and a sudden step change in load at reference velocity. Figure 9 shows the velocity response at the reference velocity 3(m/s) with no load case, and a sudden load of (200)N is added at t = (0.6)s.
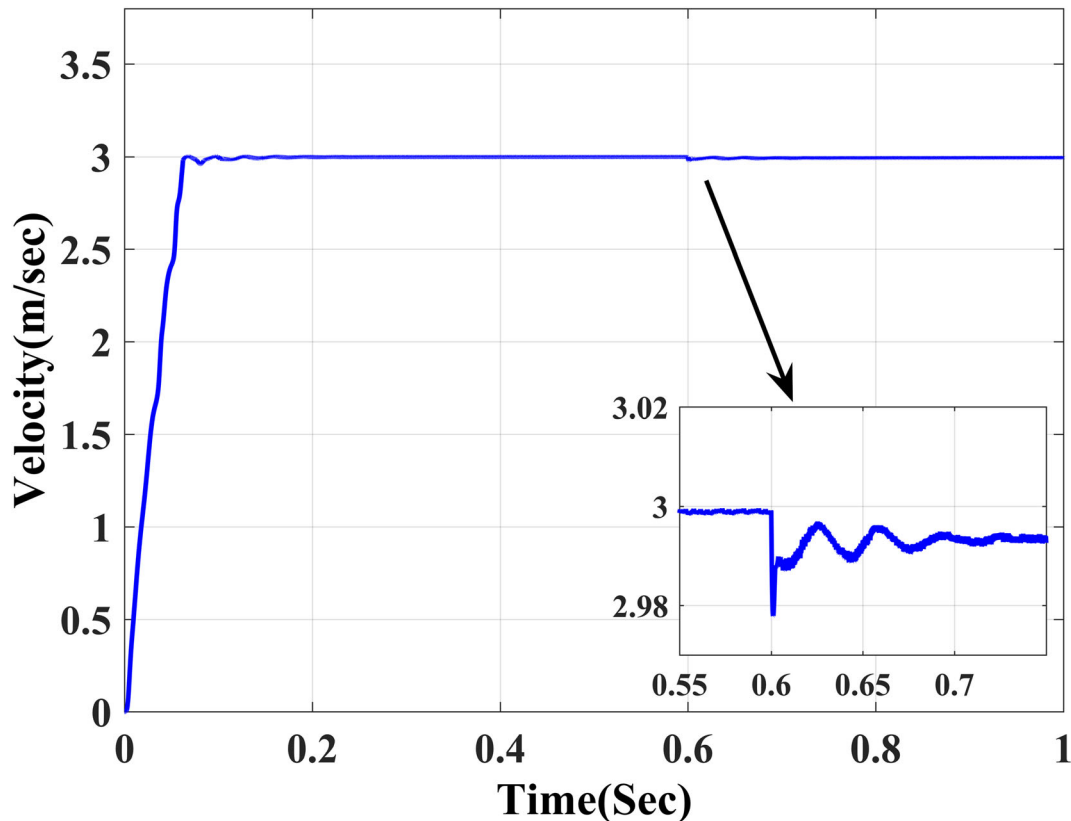
FIGURE 9 The velocity response under different cases
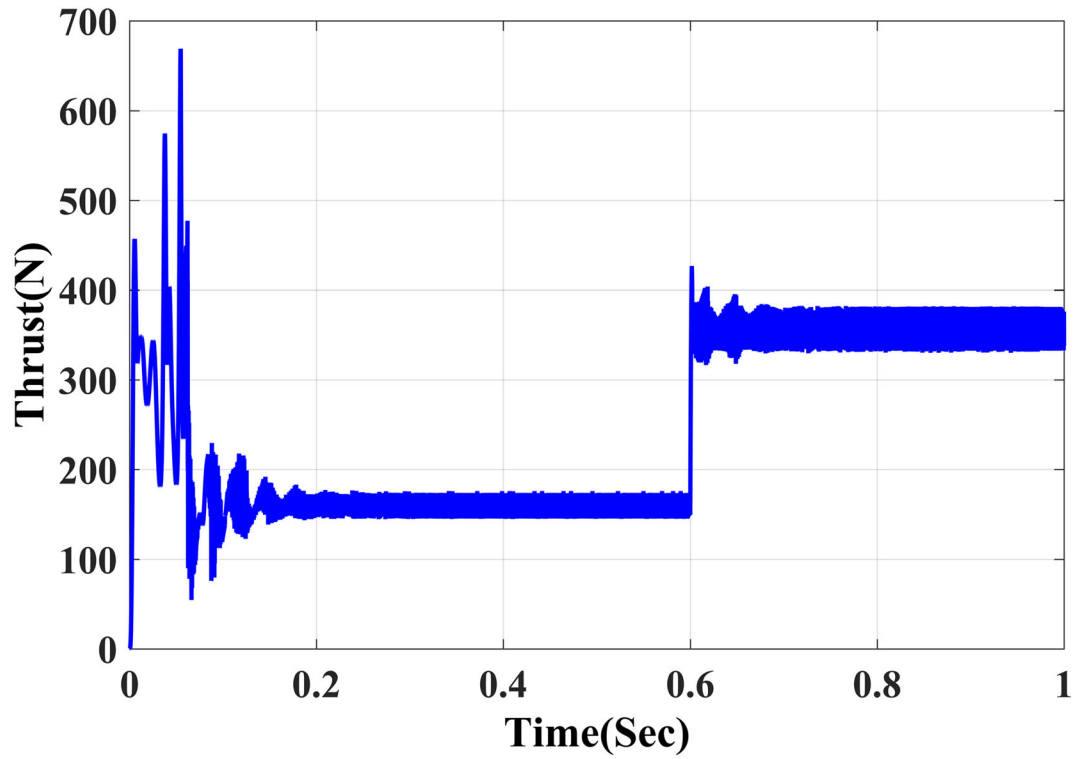
FIGURE 10 Obtained thrust force of the LIM under different cases

The established thrust during the no load and load case is illustrated in Figure 10. The components of primary current (d-q) in the paradigm no load and load are indicated in Figures 11 and 12 correspondingly Figures 13 and 14 demonstrate the secondary current components (d-q) in the case of no load and load situation. The F(Q) function
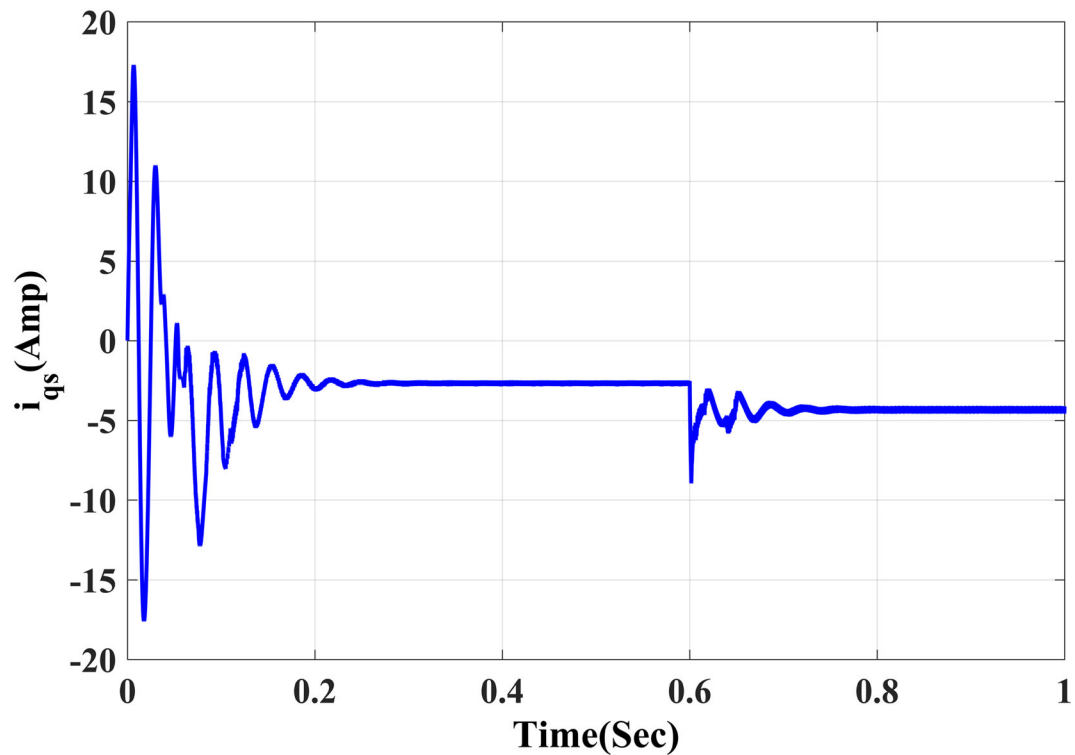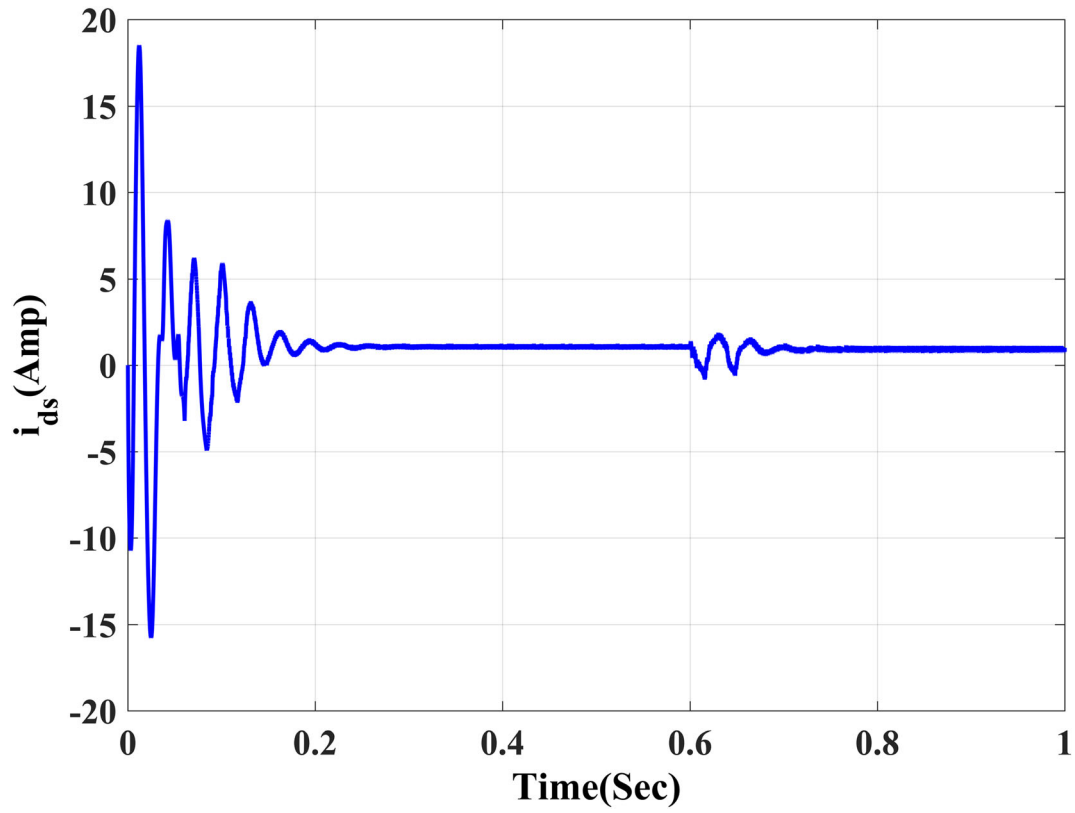

FIGURE 11 Q-axis component for primary current under different cases

FIGURE 12 D-axis component for primary current under different cases
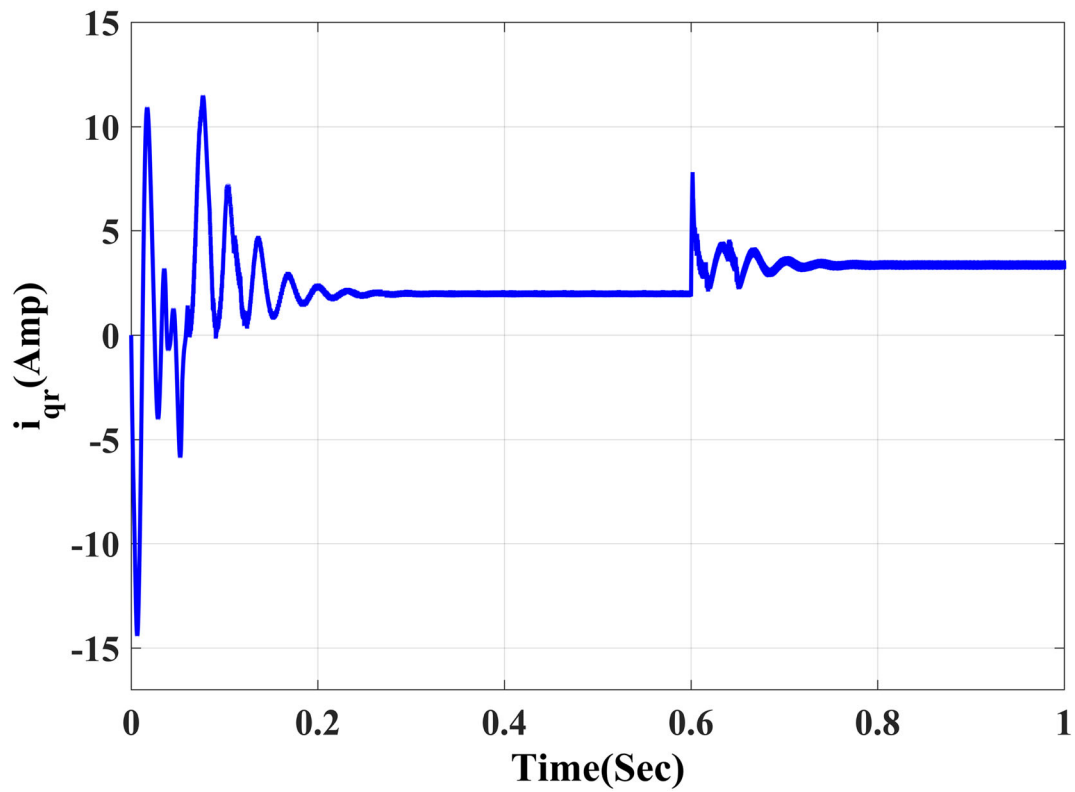
FIGURE 13 Q-axis component for secondary current under different cases
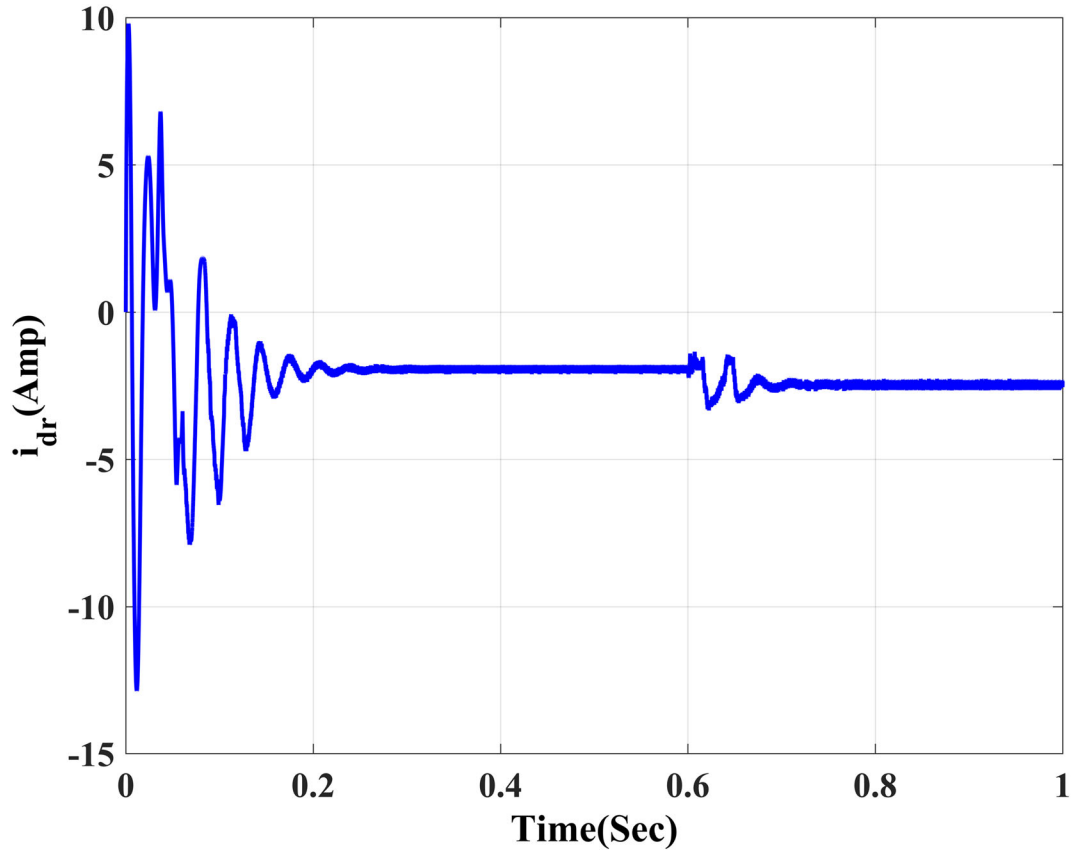
FIGURE 14 D-axis component for secondary current under different cases
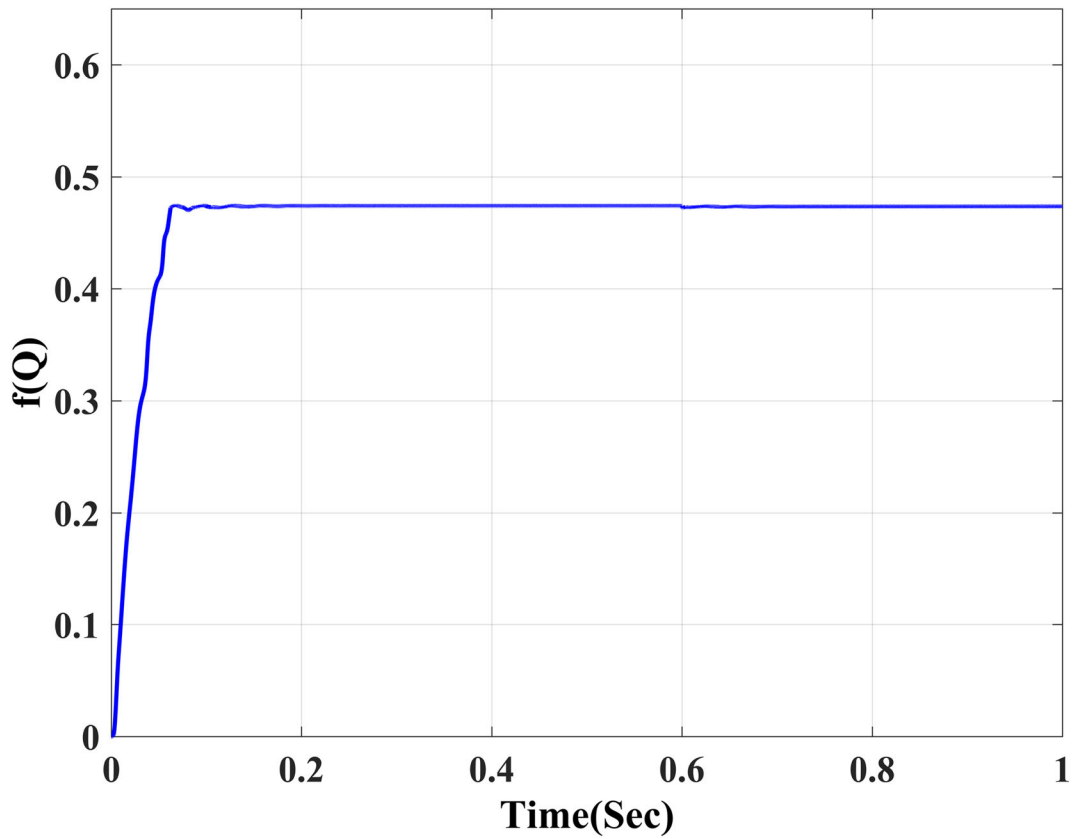

FIGURE 15 f(Q) function

for the identical beginning and loading cases is depicted in Figures 15. The step change within the obtained thrust load is at static reference velocity 3(m/s). In the case, the load is altered from no load at beginning to a sudden load of (100)N added at t = (0.4)s and rises (100)N every (0.3)s; the results are as shown in Figures 16. Figures 17
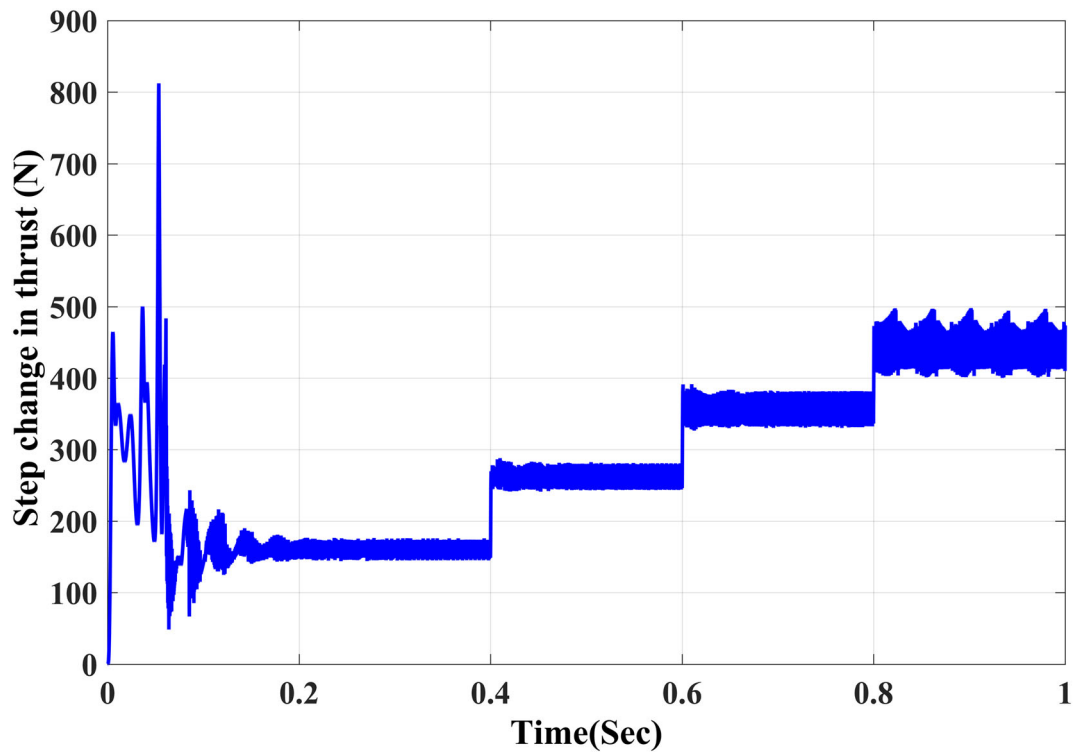

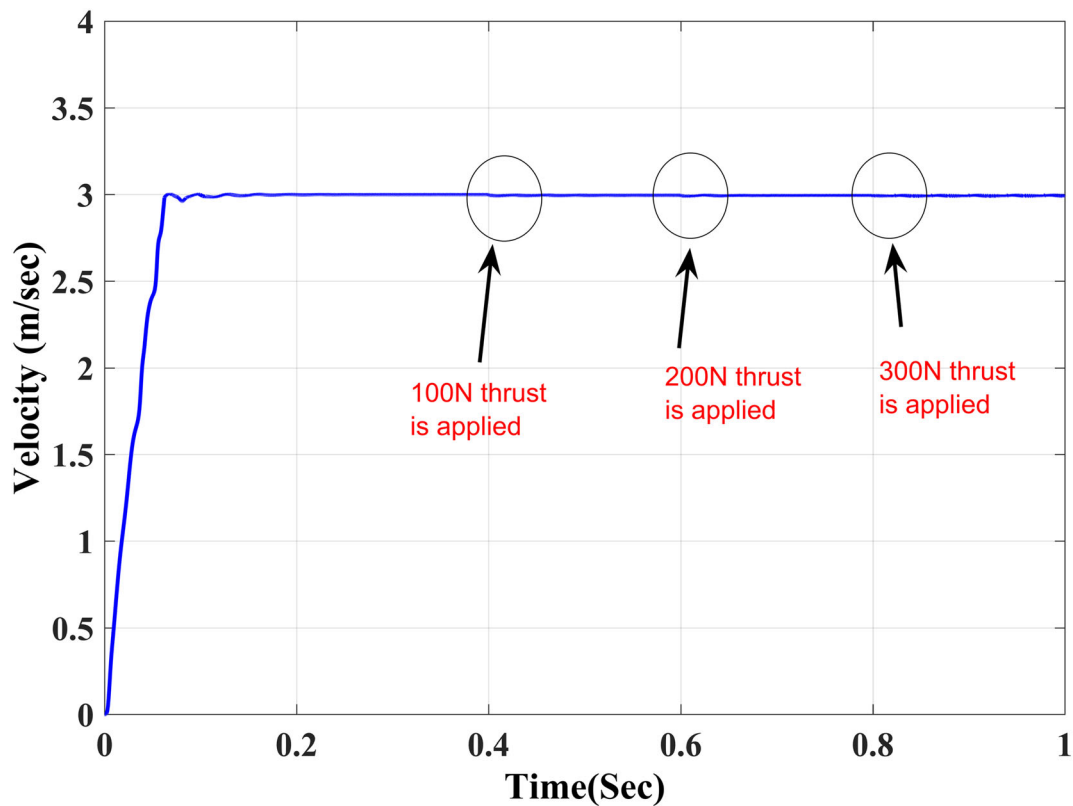
FIGURE 16 The step change in developed thrust

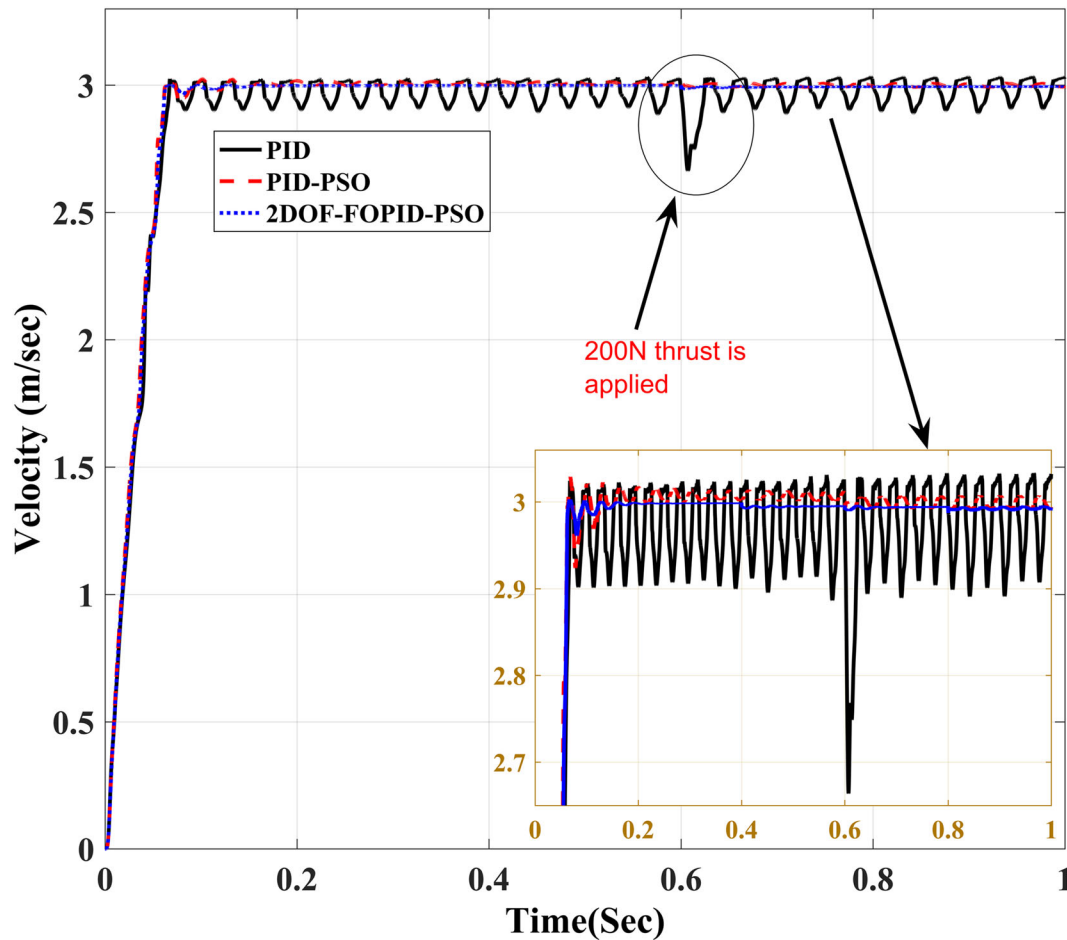**FIGURE 17** The velocity response during the step change in the thrust

FIGURE 18 The velocity response during the step change in the thrust for a different controller

indicates the response of the linear velocity through the step change in the load. Figure 18 depicts the performance comparison of the linear velocity responses for the simple PID (using Ziegler-Nichols method), PID-PSO, and 2DOF-FOPID controllers.

6 | CONCLUSION

A proposed optimal 2DOF-PI$^\lambda$D$^\mu$ controller with anti-windup technique applied to deal with the velocity of LIM has been presented. IFOC method with SVPWM inverter was utilized to achieve the required velocity and flux tracking of LIM. PSO algorithm was found suitable to utilize the tuning parameters of the proposed controllers to reach the optimal operation. It also concluded that the proposed controller was able to improve the velocity response and achieve better performance based on a flexible and robust system.

ORCID

Yasir I. A. Al-Yasir https://orcid.org/0000-0002-7859-3550

REFERENCES

1. Thomas J, Hansson A. Speed tracking of a linear induction motor-enumerative nonlinear model predictive control. *IEEE Trans Control Syst Technol.* 2013;21(5):1956-1962.
2. Wang K, Li Y, Ge Q, Shi L. Indirect field oriented control of linear induction motor based on optimized slip frequency for traction application. IEEE, 18th European Conference on Power Electronics and Applications, Karlsruhe, Germany. 2016: 1-10.

3. Yuhua W, Kang G. Speed and rotator magnetic flux close loop vector control system for the linear induction motor based on neuron adaptive controller. IEEE, International Conference on Management and Service Science. 2009: 1-5.

4. Hamedani P, Shoulaie A. Indirect field oriented control of linear induction motors considering the end effects supplied from a cascaded H-bridge inverter with multiband hysteresis modulation. IEEE, 4th Power Electronics, Drive Systems & Technologies Conference. Tehran, Iran. 2013: 13-19.

5. Hamzehbahmani H. Modeling and simulating of single side short secondary linear induction motor for high speed studies. *Int Trans Electr Energy Syst.* 2012;22(6):747-757.

6. Saleh AL, Obaid BA, Obed AA. Motion control of linear induction motor based on optimal recurrent wavelet neural network-PID controller. *Int J Eng Technol.* 2018;7(4):2028-2034.

7. Boucheta A, Bousserhane IK, Hazzab A, Mazari B, Fellah MK. Linear induction motor control using sliding mode considering the end effects. IEEE, 6th International Multi-Conference on Systems, Signals and Devices. 2009:1-6.

8. Mohamed EM, Sayed MA, Mohamed TH. Sliding mode control of linear induction motors using space vector controlled inverter. IEEE, International Conference on Renewable Energy Research and Applications. Madrid, Spain. 2013: 650-655.

9. Shadabi H, Sadat AR, Pashaei A, Sharifian MBB. Speed control of linear induction motor using DTFC method considering end-effect phenomenon. *Int J Tech Phy Prob Eng.* 2014;7:75-81.

10. Kumar KV, Michael PA, John JP, Kumar SS. Simulation and comparison of SPWM and SVPWM control for three phase inverter. *ARPN J Eng Applied Sci.* 2010;5(7):61-74.

11. Chasib AJ, Abdulabbas AK, Obed AA. Independent control of two-PMSM fed by two SVPWM inverters with fault tolerant operation. *Basrah J Eng Sci.* 2016;16(1):51-61.

12. Saleh AL, Obed AA. Speed control of brushless DC motor based on fractional order PID controller. *Int J Comput Appl.* 2014;95(4):1-6.

13. Saleh AL, Hussain MA, Klim SM. Optimal trajectory tracking control for a wheeled mobile robot using fractional order PID controller. *J University of Babylon, Eng Sci.* 2018;26(4):292-306.

14. Kadhim AK, Obed AA. Brushless DC motor speed control based on PID controller with 2-DOF and anti-windup techniques. The Second Engineering Conference for Graduate Research Middle Technical University -Electrical Engineering Technical College. Baghdad. Iraq. 2017: 1-14.

15. Shin H, Park J. Anti-windup PID controller with integral state predictor for variable-speed motor drives. *IEEE Trans Ind Electron.* 2012;59(3):1509-1516.

16. Pandey S, Dwivedi P, Junghare A. A newborn anti-windup scheme based on state prediction of fractional integrator for variable speed motor. 17th International Conference on Control, Automation and Systems. Ramada Plaza, Jeju, Korea. 2017: 663-668.

17. Padula F, Visioli A, Pagnoni M. On the anti-windup schemes for fractional-order PID controllers. IEEE International Conference on Power Electronics. Intelligent Control and Energy Systems. Delhi, India. 2016.

18. Obed AA, Saleh AL. Speed control of BLDC motor based on recurrent wavelet neural network. *Iraq J Electrical Electronic Eng.* 2014;10(2):118-129.

19. Burns RS. *Advanced Control Engineering.* Oxford: Butterworth–Heinemann; 2001:1-464.

20. Jagan NC. *Control Systems.* Second ed. Hyderabad: BS Publications/BSP Books; 2008:1-494.

21. Ogata K. *Modern Control Engineering.* Fifth ed. California: Pearson Higher Ed; 2010:1-905.

22. Jang S-M, Park Y-S, Sung S-Y. Dynamic characteristics of a linear induction motor for predicting operating performance of magnetic levitation vehicles based on electromagnetic field theory. *IEEE Trans Magn.* 2011;47(10):3673-3676.